

5. UPPER-AIR AIR QUALITY MEASUREMENTS

Aloft air quality measurements during SCOS97-NARSTO IOPs include ground-based lidar, instrumented aircraft and ozonesondes.

5.1 Ground Based Ozone Lidar

Differential Absorption Lidar (DIAL) has previously been used in a number of regional air quality studies to measure both spatial and temporal distribution of atmospheric pollutants. The pollutant of interest in most studies was ozone (O_3). Recent studies in the United States which have utilized DIAL ozone measurements include the 1991 Lake Michigan Ozone Study (LMOS) (Uthe et al., 1992), the 1993 Coastal Oxidant Assessment for Southeast Texas (COAST) study (Moosmüller, 1994; Moosmüller et al., 1994), the 1993 Los Angeles Atmospheric Free Radical Study (Zhao et al., 1994) and the 1995 Southern Oxidant Study (SOS) (Alvarez II et al., 1997). Generally, DIAL systems have been operated in these studies on an exploratory basis without formal quality assurance procedures. However, to fully utilize DIAL capabilities for the respective study purposes, well established quality assurance procedures are necessary to provide quantitative estimates of precision, accuracy, and validity of the measurements and to optimize measurement and data analysis procedures. Therefore, every effort should be made to establish an effective DIAL quality assurance program for SCOS97. It is important that the QA team does not treat the DIAL system as a “black box” for measuring ozone concentrations, but has an in-depth understanding of the measurement and data analysis process, the DIAL hardware, and the potential problems involved. The specialized nature of ozone DIAL measurements precludes simple performance audits for these measurements. Intercomparison studies are typically used to assess the accuracy and precision of DIAL measurements.

In addition to the measurement of ozone concentration profiles ozone lidars can utilize their “off channel” to monitor aerosol backscatter structures. The resulting aerosol data are extremely valuable for the visualization of atmospheric layers, but are only semi-quantitative in nature due to limitations in lidar inversion techniques.

The Atmospheric Lidar Division of NOAA’s Environmental Technology Laboratory in Boulder has developed a transportable ozone and aerosol lidar specifically for the measurement of ozone in the boundary layer and the lower free troposphere. This lidar has been employed in several field experiments:

- July 1993, Intercomparison Experiment in Davis, CA, sponsored by ARB (Zhao *et al.*, 1994)
- September 1993, LAFRS Experiment in Claremont, CA, sponsored by ARB (Zhao *et al.*, 1994)
- August, 1995, Ozone Transport Experiment in Victorville, CA, sponsored by ARB
- October–November 1995, Table Mountain Vertical Ozone Transport and Intercomparison Experiment in Boulder, CO, sponsored by NOAA.

This system is based on a solid state laser, the Nd:YAG laser with a fundamental wavelength of 1064 nm and a pulse repetition rate of up to 10 Hz. The third harmonic of this wavelength (i.e., 355 nm) with an operating pulse energy of 7–10 mJ is used for aerosol profiling with a range of about 9 km. The fourth harmonic of the fundamental (i.e., 266 nm) with an operating pulse energy of 20–30 mJ is used as “on-line” for the ozone measurement. The “off-line” for the ozone measurement is generated by Raman shifting the second harmonic (i.e., 532 nm) by the vibrational frequency of the deuterium molecule (i.e., 2987 cm⁻¹) to 632.5 nm, and subsequent sum-frequency mixing of 532 nm and 632.5 nm, yielding an “off-line” at 289 nm. The Raman shifting takes place in a specially designed Raman cell, yielding a pulse energy of 1-2 mJ at 289 nm. This process utilizes the laser energy better than the more direct Raman shifting of the fourth harmonics (Ancellet et al., 1989; Zhao et al., 1994), while yielding the same wavelength.

The receiver section utilizes an 8”-diameter telescope to collect the backscattered light. Dichroic beamsplitters separate the light from the different laser lines for the detection by photomultiplier tubes. The signals are digitized by 12 bit A/D converters for the subsequent analysis. The aerosol channel formerly had an 8 bit A/D converter which is being replaced by a 12 bit A/D converter.

Ozone measurements can be obtained for a range of up to 3 km under moderate to high surface ozone concentrations (< 150 ppb) while, for extremely high concentrations, a range of 2 km can still be achieved. The lower range limit is very good (\approx 50 m) due to the use of an innovative technique for the compression of the lidar dynamic range (Zhao et al., 1992). The measurement direction of the lidar system can be scanned in one dimension from 30° to 150° yielding a two dimensional ozone measurement.

The data quality objectives for ozone measurements with the NOAA ozone lidar are ± 5 ppb for ranges up to 1.5 km and ± 10 ppb for ranges up to 3 km for moderate to high surface ozone concentration (< 150 ppb) under the assumption of 1 min temporal and 50 m spatial averaging. The lidar observation in a 2-dimensional vertical plane will take 11 min for a scan from 30° to 150° in 10° steps, firing 100 laser shots at each angle with a pulse repetition rate of 2 Hz. If higher temporal resolution is desired the system can be operated with a pulse repetition rate of 10 Hz. Preliminary ozone data for visualization and for intercomparison with in situ sensors will be available in near real time. This ability will greatly facilitate an ozone lidar performance audit.

Successful use (i.e., meeting the quality objectives) of the NOAA ozone lidar in 2-dimensional scanning mode is contingent on improvements of the scanning system. Previous use of the system in scanning mode has yielded relatively poor quality data due to problems with thermal expansion of a scanning mirror and subsequent optical distortions. NOAA expects to have eliminated these problems and to have conducted system and performance tests prior to the system’s deployment in SCOS97.

The NOAA ozone lidar will be transported to California in June 1997 and set up at the El Monte site. During SCOS97, the lidar will gather 350 hours of data, split up into seven intensive measurement periods to capture various types of ozone episodes. When an ozone episode of interest is expected to develop, NOAA staff will fly within 24 hours to the lidar site and begin to collect data.

5.2 Instrumented Aircraft

Instrumented aircraft will be used to measure the three-dimensional distribution of ozone, ozone precursors and meteorological variables. The aircraft will provide information at the boundaries of the modeling domain and will document the vertical gradients, the mixed layer depth, and nature of the polluted layers aloft. Four aircraft are included in the core program and additional aircraft may be available for short periods. The University of California, Davis Cessna 182 will be used to characterize processes resulting in ozone layer aloft in the SoCAB and ozone fluxes into the San Fernando Valley. It will also provide data to validate the ground-based lidar measurements by NOAA at the El Monte Airport. The Sonoma Technology Piper Aztec will provide boundary and initial conditions in the northern portion of the study domain and serve as back-up to the western boundary aircraft. It will also provide data to characterize ozone and NO_y fluxes through Tehachapi and Cajon Passes and profiles in the eastern portion of the SoCAB. The Gibbs Flying Service Cessna 182 will provide initial condition in the southern portion of the modeling domain and provide data to determine the presence of pollutant transport between the SoCAB and the San Diego Air Basin. The EOPACE aircraft will provide boundary and initial conditions in the western (over-water) region of the modeling domain and provide data on any offshore movement of pollutants from the SoCAB.

5.2.1 UCD Airborne Instrumentation (UCD Cessna 182, Gibbs Cessna 206)

Air quality instrumentation provided by Dr. John J. Carroll of the University of California at Davis (UCD) will be utilized in two aircraft, UCD Cessna 182 and Gibbs Flying Service Cessna 206. The instrumentation has been used in the UCD C-182 for several years. It is being duplicated and installed onboard the Gibbs Flying Service Cessna 206. The air quality instrumentation onboard this aircraft will be maintained and calibrated by the San Diego Air Pollution Control District (SDAPCD). An overview of the UCD instrumentation complete with data quality objectives, i.e., accuracy is given in Table 5-1.

The UCD aircraft will be used to investigate up to seven ozone episodes. During each episode of interest the aircraft will be based at the El Monte Airport (close vicinity to NOAA lidar) and will operate for three days. Each day, three flights consisting of up to four vertical spirals (460 to 3,050 m MSL) will be conducted. On selected days, a fourth flight consisting of two spirals will be made. The Gibbs Cessna will be based at Montgomery Field in San Diego. It will make two flight on IOP days consisting of up to five spirals.

System performance checks will be done daily and calibrations will be performed before and after each operational period. Each day's data will be screened as it is collected to check the performance of each component.

Table 0-1
UCD Instrumentation

Parameter Measured	Technique	Manufacturer	Time Response	Measurement Range	Accuracy
Pressure (Altitude)	Capacitive	Setra	1 s - 3 s	-30 m - 3700 m	± 0.3 mB ± 3 m
Temperature	Platinum RTD	Omega	1 s - 3 s	-20°C - 50°C	$\pm 0.2^\circ\text{C}$
Relative Humidity	Capacitive	Qualimetrics	1 s - 3 s	10% - 98%	$\pm 3\%$
Air Speed	Thermal Anemometer	T.S.I.	1 s - 3 s	15 m/s - 75 m/s	± 0.4 m/s
Heading	Electronic Compass	Precision Navigation	1 s - 3 s	0° - 359°	$\pm 2^\circ$
Position	GPS	Garmin	10 s	Lat. - Long.	± 15 m
Particle Concentration	Optical Counter	Climet	10 s	2 channels: d > 0.3 μm & d > 3 μm	$\pm 2\%$
NO, NO ₂ Concentration	O ₃ Titration Chemilumin.	Monitor Labs.	10 s - 15 s	0 ppmv - 20 ppmv	± 0.5 ppbv
Ozone Concentration	UV Absorption	Dasibi 1008	10 s - 15 s	0 ppbv - 999 ppbv	± 3 ppbv

5.2.2 STI Airborne Instrumentation (STI Piper Aztec)

Sonoma Technology, Inc. (STI) will use its instrumented twin-engine Piper Aztec aircraft for this study. The onboard instrumentation can measure continuously ozone, NO, NO_y, b_{scat}, position, temperature, dew point, turbulence, and one of SO₂, CO, or NO_y minus nitric acid and aerosol nitrate (NO_w). The NO/NO_y, NO_w, SO₂, and CO instruments are high-sensitivity instruments, capable of measuring background concentrations likely to be observed in the study area. An overview of the STI instrumentation complete with data quality objectives, i.e., accuracy is given in Table 5-2.

The STI aircraft will be based at Camarillo and about 38 flights (150 flight hours) will be conducted over 15 to 20 days during the study period. The aircraft will be available for two flights a day for up to four days in a row. On a few selected days three flights per day can be conducted.

Instrument calibrations will be performed before and after each flight day. This makes it possible to immediately identify and correct problems and to know which data are affected. Some potential instrument problems are not identified by calibration. Therefore flight data will be reviewed in the field on a daily basis.

Table 0-2
STI Instrumentation

Parameter Measured	Technique	Manufacturer	Time Response	Measurement Range(s)	Accuracy^a (Full Range)
NO/NO _y Concentration	Chemilumin.	Thermo Env. Model 42S	< 20 s	50 ppb, 100 ppb, 200 ppb	± 10%
Ozone Concentration	Chemilumin.	Monitor Labs. 8410E	12 s	200 ppb, 500 ppb	± 10%
b _{scat}	Integrating Nephelometer	MRI 1560 Series	1 s	100 Mm ⁻¹ , 1000 Mm ⁻¹	± 10%
Dew Point	Cooled Mirror	Cambridge Systems 137-C	0.5 s/°C	-50°C - 50°C	± 10%
Altitude	Altitude Encoder	II-Morrow	1 s	0 m - 5000 m	± 10%
Altitude (backup)	Pressure Transducer	Validyne P24	< 1 s	0 m - 5000 m	± 10%
Temperature	Bead Thermistor/ Vortex Housing	YSI/MRI	5 s	-30°C - 50°C	± 10%
Temperature (backup)	Platinum Resistance	Rosemont 102 AV/AF	1 s	-50°C - 50°C	± 10%
Position	GPS	II-Morrow	< 1 s	Lat. - Long.	± 50 m
Data Logger (includes time)	Dual Floppy Acquisition	STI 486 System	1 s	± 9.99 VDC	± 10%
NO/NO _w ^b	Chemilumin.	Thermo Env. Model 42S	< 20 s	50 ppb, 100 ppb, 200 ppb	± 10%
SO ₂ ^b	Pulsed Fluorescence	Thermo Env. Model 43S	15 s	1 ppb, 5ppb, 50 ppb, 200 ppb	± 10%
CO ^b	Gas Filter Correlation	Thermo Env. Model 48S	< 20 s	1 ppm, 2 ppm, 5 ppm, 10 ppm	± 10%

^a For values between 10% and 90% of full scale

^b Without modifying the aircraft for additional power, only one of these three instruments can be operated.

5.2.3 Navy EOPACE Airborne Instrumentation (Gibbs Piper Navajo)

The Navy EOPACE aircraft will be instrumented with an UV absorption instrument (Dasibi) for the measurement of ozone concentrations, four canisters for hydrocarbon sampling, three tedlar bags for carbonyl sampling and ancillary instrumentation for the measurement of temperature, relative humidity, and position. Position will be determined with a GPS instrument and a pressure (altitude) monitor. Further details and data quality objectives are currently not available.

5.2.4 Ancillary Instrumentation

Ancillary airborne instrumentation includes navigational instruments measuring quantities such as position, altitude, heading, and time, and instruments which determine additional atmospheric properties such as temperature, humidity, and aerosol characteristics. Some of the instruments used to measure these quantities on SCOS97 air quality aircraft are briefly described in the following.

5.2.5 Navigational Instruments

Position of the airborne platform in space and time is extremely important for the use and intercomparison of all other measured quantities. The Global Positioning System (GPS), a satellite system operated by the U.S. Department of Defense (DOD) provides radio signals from which GPS receivers can calculate 3-dimensional position and time at several different accuracy levels.

Civilian users worldwide use the Standard Positioning System (SPS) without charge or restrictions. Most receivers are capable of receiving and using the SPS signal. The SPS accuracy is intentionally degraded by the DOD by the use of Selective Availability (SA). The SPS predictable accuracies are: 100 m horizontal accuracy, 156 m vertical accuracy, and 340 ns time accuracy. These GPS accuracy figures are from the 1994 Federal Radionavigation Plan. The figures are 95% accuracies, and express the value of two standard deviations of radial error from the actual antenna position to an ensemble of position estimates made under specified satellite elevation angle (five degrees) and Position Dilution of Precision PDOP (less than six) conditions. For horizontal accuracy figures 95% is the equivalent of 2drms (two-distance root-mean-squared), or twice the radial error standard deviation. For vertical and time errors 95% is the value of two-standard deviations of vertical error or time error. Receiver manufacturers may use other accuracy measures. Root-mean-square (RMS) error is the value of one standard deviation (68%) of the error in one, two or three dimensions. Circular Error Probable (CEP) is the value of the radius of a circle, centered at the actual position that contains 50% of the position estimates. Spherical Error Probable (SEP) is the spherical equivalent of CEP, that is the radius of a sphere, centered at the actual position, that contains 50% of the three dimension position estimates. As opposed to 2drms, drms, or RMS figures, CEP and SEP are not affected by large blunder errors making them an overly optimistic accuracy measure. Some receiver specification sheets list horizontal accuracy in RMS or CEP and without Selective Availability, making those receivers appear more accurate than those specified by more responsible vendors using more conservative error measures.

Authorized users with cryptographic equipment and keys and specially equipped receivers use the Precise Positioning System (PPS). U.S. and Allied military, certain U.S. Government agencies, and selected civilian users specifically approved by the U. S. Government, can use the PPS. The PPS predictable accuracies are: 22 m horizontal accuracy, 27.7 m vertical accuracy, and 100 ns time accuracy.

Differential GPS (DGPS) techniques improve the accuracy of GPS by correcting bias errors at one location with measured bias errors at a known position. A reference receiver, or base station, computes corrections for each satellite signal. Because individual pseudo-ranges must be corrected prior to the formation of a navigation solution, DGPS implementations require software in the reference receiver that can track all satellites in view and form individual pseudo-range corrections for each satellite. These corrections are passed to the remote, or rover receiver which must be capable of applying these individual pseudo-range corrections to each satellite used in the navigation solution. Applying a simple position correction from the reference receiver to the remote receiver has limited effect at useful ranges because both receivers would have to be using the same set of satellites in their navigation solutions and have identical Geometric Dilution of Precision (GDOP) terms (not possible at different locations) to be identically affected by bias errors. Differential corrections may be used in real-time or later, with post-processing techniques. Real-time corrections can be transmitted by radio link. The U. S. Coast Guard maintains a network of differential monitors and transmits DGPS corrections over radio beacons covering much of the U. S. coastline. DGPS corrections are often transmitted in a standard format specified by the Radio Technical Commission Marine (RTCM). Corrections can be recorded for post processing. Many public and private agencies record DGPS corrections for distribution by electronic means. Private DGPS services use leased FM sub-carrier broadcasts, satellite links, or private radio-beacons for real-time applications. To remove Selective Availability (and other bias errors), differential corrections should be computed at the reference station and applied at the remote receiver at an update rate that is less than the correlation time of SA. Suggested DGPS update rates are usually less than twenty seconds. DGPS removes common-mode errors, those errors common to both the reference and remote receivers (not multipath or receiver noise). Errors are more often common-mode when receivers are close together (less than 100 km). Differential position accuracies of 1-10 meters are possible with DGPS.

An extensive overview of the GPS system and further references have been given by Dr. Peter H. Dana of the University of Texas at Austin and can be found on his web site at <http://www.utexas.edu/depts/grg/gcraft/notes/gps/gps.html>.

The vertical accuracy of standard GPS (156 m for SPS) is marginal for lower tropospheric studies. Therefore, vertical position, i.e., altitude is often derived from pressure measurements. If the pressure-derived altitude measurement is corrected for atmospheric pressure changes before take-off and/or after landing an accuracy of ± 3 m can be obtained.

5.2.6 Temperature Measurement

Temperature can be measured via a diverse array of sensors. All of them infer temperature by sensing some change in a physical characteristic. Resistive temperature devices (RTDs and thermistors) are commonly used to measure air temperature in conjunction with a data acquisition system.

Resistive temperature devices capitalize on the fact that the electrical resistance of a material changes as its temperature changes. Two key types are the metallic devices (commonly referred to as RTDs), and thermistors. As their name indicates, RTDs rely on resistance change in a metal, with the resistance rising more or less linearly with temperature. Thermistors are based on resistance change in a ceramic semiconductor; the resistance drops nonlinearly with temperature rise.

A typical RTD consists of a fine platinum wire wrapped around a mandrel and covered with a protective coating. Usually, the mandrel and coating are glass or ceramic. The mean slope of the resistance versus temperature plot for the RTD is often referred to as the alpha value, alpha standing for the temperature coefficient. The slope of the curve for a given sensor depends somewhat on purity of the platinum in it. The most commonly used standard slope, pertaining to platinum of a particular purity and composition, has a value of 0.00385 (assuming that the resistance is measured in ohms and the temperature in degrees Celsius). A resistance versus temperature curve drawn with this slope is a so-called European curve, because RTDs of this composition were first used extensively on that continent. Complicating the picture, there is also another standard slope, pertaining to a slightly different platinum composition. Having a slightly higher alpha value of 0.00392, it follows what is known as the American curve. If the alpha value for a given RTD is not specified, it is usually 0.00385. However, it is prudent to make sure of this, especially if the temperatures to be measured are high.

The resistance-temperature relationship of a thermistor is negative and highly nonlinear. This poses a serious problem for engineers who must design their own circuitry. However, the difficulty can be eased by using thermistors in matched pairs, in such a way that the nonlinearities offset each other. Furthermore, vendors offer panel meters and controllers that compensate internally for thermistors' lack of linearity. Thermistors are usually designated in accordance with their resistance at 25°C. The most common of these ratings is 2252 Ω ; among the others are 5,000 Ω and 10,000 Ω . If not specified to the contrary, most instruments will accept the 2252 Ω type of thermistor.

5.2.7 Humidity Measurement

The humidity of air can be expressed as absolute humidity (either dew point or water concentration) or relative humidity. These quantities can easily be converted from one to the other if the atmospheric temperature is known. Two common methods of measuring atmospheric humidity are described in the following.

The dewpoint monitor determines absolute humidity from a fundamental measurement and therefore does not depend on empirical calibration factors. This instrument cools a small mirror to the point at which moisture condenses on the mirror surface and optically detects the first sign of condensation. The mirror temperature is measured accurately, often with an RTD resulting in a measurement of the dewpoint which is directly related to the absolute humidity.

The capacitive humidity sensor measures relative humidity via the change in capacity of a thin film polymer capacitor. The thin polymer film either absorbs or exudes water vapor as the relative humidity of the ambient air rises or drops. The dielectric properties of the polymer film depend on the amount of water contained in it: as the relative humidity changes, the dielectric

properties of the film change and so the capacitance of the sensor changes. The electronics of the instrument measure the capacitance of the sensor and converts it into a humidity reading.

5.3 Ozonesondes

The objective of the ozonesonde program is to collect, validate and report vertical profiles of oxidant concentration, temperature, and humidity four times per day at each of six monitoring locations on 15 intensive operating period days, and to characterize these data with respect to precision and accuracy. The primary data quality objective for this project is 100% valid data capture for the resulting 360 oxidant profiles. To be considered valid, the profiles must meet specified tolerances for place and time of collection, for vertical extent and resolution, and for precision and accuracy.

The general locations of ozonesonde launch sites and the rationale for their location are as follows:

- Van Nuys Airport: monitor ozone aloft in the San Fernando Valley that may contribute to transport through Thousand Oaks, Simi Valley, or Newhall.
- Downtown Los Angeles: monitor southern extent of recirculation from the San Gabriel Mountains or recirculation from the ocean.
- Anaheim: monitor transport into San Diego County, and monitor recirculation from the ocean.
- Upland/Ontario: monitor transport and recirculation between the coastal plain and the low desert.
- Riverside: monitor ozone aloft in the low desert that may contribute to transport through the Banning Pass.
- North County/Escondido: monitor overland transport from SoCAB into San Diego County.

CE-CERT has established tentative data quality indicators (DQI) and goals for the ozonesonde instrumentation. Data quality indicators and goals for ozonesondes and the associated meteorological instruments are summarized in Tables 5-3 and 5-4, respectively.

The accuracy of the ozonesondes is mainly limited by the large interference bias of -10 ppb to +50 ppb. If the concentration range of interferents can be estimated it may be possible to reduce the interference bias.

Table 0-3: CE-CERT Ozonesonde, Data Quality Indicators and Goals

DQI	Goal
Precision	1-sigma < larger of 5 ppb or 10%
Calibration Bias	1-sigma < larger of 5 ppb or 10%
Interference Bias	-10 to + 50 ppb
Lower Quantifiable Limit	< 15 ppb
Response Time	> 80% of step change in 1 minute
Ascent Rate	< 3.0 m/s
Response Distance	> 80% in 180 meters
Time of Launch	+/- 3.0 hours from planned time
Location of Launch	+/- 100 meters from planned location
Duration of Flight	>3000 meters AGL

Table 0-4: CE-CERT Meteorological Instruments, Data Quality Indicators and Goals

Measurement	DQI	Goal
Temperature	Precision	$\pm 1\text{ }^{\circ}\text{C}$
Temperature	Calibration Bias	$\pm 3\text{ }^{\circ}\text{C}$
Temperature	Response Time	> 63% response in 20 s
Pressure	Precision	$\pm 2\text{ mb}$
Pressure	Calibration Bias	$\pm 5\text{ mb}$
Pressure	Response Time	> 63% response in 2 s
Relative Humidity	Precision	$\pm 5\%\text{ RH}$
Relative Humidity	Calibration Bias	$\pm 10\%\text{ RH}$
Relative Humidity	Response Time	> 63% response in 2 min

5.4 System Audits

5.4.1 Some Aspects of Ozone Lidar System Audits

Both accuracy and precision of ozone DIAL measurements are multi-dimensional functions of the specific DIAL system used, the measurement distance, spatial and temporal resolution of the ozone measurement, and of atmospheric conditions such as ozone and aerosol concentration, properties, and distribution. It is the task of the DIAL contractor to determine a useful approximation to this function. This information can then be used, prior to field operations, to decide on some of the standard operating and data analysis procedures. As these procedures are dependent on the desired accuracy, precision, and spatial and temporal resolution, they should not be determined by the DIAL contractor alone. Instead they ought to be the result of discussions between data users, DIAL contractor, and QA team.

The accuracy of ozone DIAL measurements is limited by both statistical and systematic errors. Statistical errors can be reduced by averaging, thereby improving precision and potentially also accuracy. However, as standard samples cannot be used, it is not trivial to distinguish between statistical errors and atmospheric fluctuations. Systematic errors are due to both the system itself and due to atmospheric conditions. Both types of error sources are discussed in the following sections.

The consideration of all error sources together with the accuracy, precision, spatial and temporal resolution goals for SCOS97 should result in standard operating procedures for the operation of the DIAL system during SCOS97 and for the subsequent data analysis. While the main data analysis will undoubtedly take place after the end of the SCOS97 measurement program, it is important that some data analysis takes place either in real time or at least on a daily basis. This will allow some direct intercomparison and performance testing to uncover possible DIAL system malfunction.

Systematic Errors due to DIAL Hardware

The lidar return signal, as described by the lidar equation, drops off dramatically with increasing range r . This drop off is due to three factors:

1. The $1/r^2$ drop off is due to the decreasing solid angle of the telescope aperture as seen from the backscattering location r , i.e., the fraction of the backscattered light collected by the telescope decreases as $1/r^2$.
2. The exponential signal drop off as a function of r is due to atmospheric extinction, i.e., both scattering and absorption. This drop off is especially serious for high aerosol loading and, below a wavelength of 300 nm, for high ozone concentrations.
3. For an upward pointing lidar system the backscatter coefficient $\beta(r)$ generally decreases with altitude due to both smaller aerosol and air density.

The rapid signal drop off with range results in a large dynamic range of the measured lidar signals, especially if measurements close to the system are of importance. This is usually the case

for air pollution studies such as SCOS97. The large dynamic signal range can result in a number of hardware related systematic errors such as

- Quantization errors result from the limited range of Analog-to-Digital (A/D) Converters used to digitize the signal from the light detector (photomultiplier). State of the art A/D converters which are fast enough to yield a spatial resolution on the order of 10 m (i.e. 67 ns) commonly have a resolution of 12 bit, they are able to cover a dynamic range of $2^{12} = 4096$. To fully exploit this dynamic range, the photomultiplier high voltage and the analog system gain have to be set appropriately to ensure that the maximum signal closely corresponds to the maximum input of the A/D converter. In addition, A/D converter nonlinearities may also be present (Langford, 1995).
- Photomultiplier tube (PMT) linearity should be comparable to, or preferable less than the quantization error of the A/D converter. For a 12 bit system, variations in both signal gain and signal linearity should be better than about 0.1%, a non trivial objective (Lee et al., 1990; Bristow et al., 1995).
- In the ultraviolet spectral region fluorescence from optical components can also cause errors near the far end of the DIAL range (Kempfer et al., 1994).

To reduce the dynamic range of the DIAL signals a number of methods have been tried. Examples are multibeam transmitters (Zhao et al., 1992), multiple telescopes and PMTs (e.g., Kempfer et al., 1994), PMT gain switching (Kempfer et al., 1994), PMT r^2 -gain modulation (Bundy, 1992), logarithmic amplifiers (e.g., Optech Systems Corporation), etc. Of course the linearity of these dynamic range reduction techniques also has to be high enough, which is not always the case.

Other potential error sources include the suppression or subtraction of background light in the near UV, optical crosstalk between different receiver channels, and electronic interference by the laser itself. These error sources are some of the more common problems. Each potential error source has to be eliminated or carefully characterized in its influence on the final measurement accuracy and precision under a range of operating conditions.

Systematic Errors due to Aerosol Extinction and Backscattering

In the planetary boundary layer, aerosol scattering can not be neglected and strong aerosol gradients occur frequently. Therefore both the extinction and backscattering corrections in the DIAL equation have to be evaluated for aerosol. It has been shown (Browell et al., 1985) that the extinction correction is on the order of only a few ppb. In regions of spatially inhomogeneous aerosol, the main correction term comes from the backscattering correction. This term can be calculated by retrieving the aerosol distribution from the off-line lidar signal and assuming an Ångström coefficient (Ångström, 1929; Völger et al., 1996) to describe the wavelength dependence of the aerosol backscatter coefficient. It should be noted that the retrieval of the aerosol distribution depends on assumptions of a boundary value at some calibration height towards the far range of the system and of the scattering phase function. The calculation of both extinction and backscattering corrections has been described in detail in a number of publications (e.g., Pelon and Mégie, 1982; Browell et al., 1985; Milton, 1987; Papayannis et al., 1990;

Kovalev and McElroy, 1994; Völger et al., 1996). In conclusion, the calculation of the aerosol corrections in the DIAL equation has potential for sizable errors. The output of the DIAL data processing should therefore include both uncorrected and corrected ozone concentration profiles and in addition the retrieved aerosol profile.

Systematic Errors due to DIAL Algorithms and Software

While the DIAL equation itself is an unequivocal mathematical expression, it describes the measured quantities as continuous functions. In reality however, only a limited number of data points are available. To device DIAL algorithms from the DIAL equation it has to be decided how to process (i.e., average, take derivatives, etc.) these discrete data points. For example the seemingly trivial issue of averaging data from multiple laser pulses is in reality quite complex (Milton and Woods, 1987). These difficulties have been expressed previously (Kempfer et al., 1994): “Perhaps the most difficult task of the lidar (referring to ozone DIAL) development has been to prepare the computer program for the data evaluation.” The resulting software tends to be complex and it is advisable to subject it to separate performance testing. This can be done by writing a program which calculates DIAL signals for a variety of model atmospheres. These “fake” signals can then be used as test input to the data analysis program.

The complete, well documented data analysis software and some results of its performance testing should become a part of the system documentation. Version upgrades should implement and document software changes and any processed data must include the version number of the processing software.

Statistical Errors

Statistical errors result from random fluctuations in the measurement both due hardware induced noise such as electronic noise and quantization noise, and the more basic shot noise resulting from quantum statistics of detected photons and of photoelectrons emitted by the photocathode in the PMT. These errors can be reduced by both spatial (in beam direction) and temporal (over many laser pulses) averaging resulting in increased measurement precision at a given distance and in increased useful measurement range at a given precision. However, averaging also suppresses potentially interesting fine structure of the atmospheric ozone concentration, both in space and time. These trade-offs should be evaluated in conjunction with the desired data accuracy and desired spatial and temporal resolution as a function of measurement distance (e.g., height above ground) and atmospheric conditions. If the DIAL system is not pointed in a fixed direction, but operated in scanning mode, the scanning pattern becomes an additional variable. It is important that this part of the standard operating and analysis procedures is determined in discussion between DIAL contractor and DIAL data users, prior to field operations. In the past, these decisions have frequently been left to the DIAL contractor. Therefore, the resulting DIAL ozone data have not been optimized for their intended use.

5.4.2 Ozone Lidar System Audits

A first system audit should take place well before the start of the SCOS97 field measurement program to leave sufficient time to correct possible deficiencies of the system and its operational and quality control procedures. This audit should include a review of system design,

operation, data analysis procedures including quality control procedures, and if possible, results of a previous performance audit. If major problems are discovered, a second audit should confirm the correction of these problems before measurements commence. A final system audit should be planned during a DIAL data acquisition period in SCOS97 to ensure the proper operation according to the standard operating procedures. At this point the QA team should already be intimately familiar with the DIAL system, its operation, and its data analysis procedures.

In reality, ozone lidar systems are prototypes, generally operated by the scientists which designed and built the system. Standard operating procedures often do not exist and may be less important as the operators are intimately familiar with their system. Effective ozone lidar system audits, as discussed above, are quite involved requiring extensive lidar expertise and time commitment. At this point (March 1997) it seems rather unlikely that an ozone lidar system audit will take place for SCOS97.

5.4.3 Aircraft Based *in Situ* Instrumentation

The systems audit of the aircraft will be done at the level of the Comprehensive Site Survey as described in Section 4.6 by personnel from the Quality Assurance (QAS) of ARB at the time the performance audits are done. The sampling procedures will be reviewed including operating procedures, calibration equipment and standards, and instrumentation. An additional review of the sampling and measurement systems will be made during the period of the aircraft intercomparisons to ensure that ambient air samples are collected and measured without bias.

5.4.4 Ozonesondes

The systems audit of the CE-CERT ozonesonde will review available test reports and standard operating procedures (SOP). This will include documentation on the ozone transfer standard used to calibrate and test the sondes and its traceability, the testing procedures, and the routine operating procedures. The release site locations will be confirmed. At least two sites will be visited and the operations observed to see if standard procedures are being followed.

5.5 Performance Audits

5.5.1 Ground Based Performance Audits

Performance audits of instruments installed on the aircraft will be conducted by personnel from Quality Assurance (QAS) of the ARB. Each measurement method will be audited on the project. The CE-CERT ozonesonde will also be audited.

As with the surface monitoring stations, performance audits are quantitative assessments of instrument operation that are accomplished by challenging site instruments with known audit standards. The procedures described in Section 4.7 for instruments at the surface sites will be followed for the aircraft equipment in as far as they are applicable. Some modifications may have to be made. The delivery of the audit gases may have to be changed to match the instrument sample inlets. The higher

ranges of audit concentrations likely exceed the operating range of the aircraft instruments. At the low concentration end, the lowest audit concentrations should be as low as possible.

Ozone concentrations will be introduced to representative number of the ozonesondes. At least 3 sondes should be used. The procedures for introducing gas to the surface analyzers will be followed although the range of points may differ some. The audit concentrations will be compared to the telemetered data.

Meteorological instrumentation on the aircraft will also be audited. The audit criteria will have to be relaxed for those instruments that require air flow past them at speeds attained by the aircraft. The measurements of temperature and relative humidity are particularly affected by the moving and static air streams. For instruments that depend on orientation during flight, such as a solar radiation sensor, the audit sensor will have to be positioned in approximately the same orientation as the aircraft sensor which may not be horizontal when the aircraft is on the ground.

All audit results will be entered on QA Audit Station Data Worksheet forms and into an audit computer. Calculations are done by the computer and by hand for verification. Preliminary results will be summarized in reports for each measurement issued to the site operator at the conclusion of the audit. For gas analyzers, the reports will present the audit concentrations, the instrument responses, and the percent differences. Instrument performance will be assessed by comparing the percent differences to EPA criteria as shown in Table 4-5. For meteorological equipment, the reports will present the expected instrument responses, the actual instrument responses, and their differences. Instrument performance will be assessed by comparing the differences to the EPA criteria as shown in Table 4-5, although possible modified as indicated above. For those instruments that exceed the criteria, the auditor will issue an Air Quality Data Action (AQDA). The site operator will be required to respond to the AQDA by detailing the actions done to correct instrumental problems found during the audit.

5.5.2 Ozone Lidar Performance Audits

A minimum of two performance audits should take place, one well before the start of the SCOS97 field measurement program. For established ozone DIAL systems like the ground based NOAA system it is likely that a previous performance audit can be used for this purpose. The second performance audit should take place during or just before the SCOS97 field program when additional intercomparison measurements are available. In addition, this audit will be more realistic taking place under atmospheric conditions comparable to those during the intensive operating periods. The actual performance audit will take the form of an intercomparison study as discussed in the following.

It is virtually impossible to test an ozone DIAL system with a standard sample under realistic, atmospheric conditions. While samples contained in a chamber have been used to calibrate some DIAL systems (e.g., Grant et al., 1974), aerosol concentrations, gradients, and size distributions, which have an important influence on ozone DIAL measurements, are much harder to control on the needed scale. Therefore, the best solution is an intercomparison study, which characterizes the DIAL measurement volume with a NIST traceable, *in situ* instrument under a

variety of realistic atmospheric conditions. Previous intercomparison studies between tropospheric, ground based ozone DIALs and *in situ* instruments include

- Ground based testing of the U.S. EPA (now NOAA ETL) airborne ozone DIAL including near horizontal pointing intercomparison with surface measurements by an ultraviolet analyzer (Moosmüller et al., 1992).
- A joint experiment (TROLIX '91), where four ozone DIAL systems from RIVM Bilthoven, MPI Hamburg, SA/CNRS Paris, and LTH Lund were compared against each other, and to ECC-sondes and ultraviolet analyzer carried by a helicopter. In addition, horizontally pointing intercomparisons were performed for two of the lidars, surface measurement by ultraviolet analyzers, and a dual-path DOAS system (Bösenberg et al., 1993).
- An intercomparison experiment between the NOAA ETL ground based ozone DIAL and an airplane based ultraviolet analyzer (Zhao et al., 1994).
- Two dedicated intercomparison campaigns between lidar, electrochemical sondes, and airborne ultraviolet analyzer in the upper troposphere and stratosphere (Beekmann et al., 1994).
- Intercomparisons between the Fraunhofer Institute ozone DIAL and nearby mountain stations, ECC-sondes, and instrumented aircraft (Kempfer et al., 1994).
- An intercomparison experiment between the MPI Hamburg ozone DIAL and ECC-sondes attached to both tethered and free flying balloons (Grabbe et al., 1996).
- The Table Mountain vertical ozone transport and intercomparison experiment. An intercomparison between NOAA ETL ground based and airborne (in ground based operation) ozone lidars. Additional intercomparison with an ground based ultraviolet analyzer for near horizontal paths (Alvarez II, 1996).

It should be kept in mind that the value of horizontal intercomparisons is limited, because aerosol interference is generally negligible for horizontal lidar measurements. For intercomparisons with vertical, or near vertical pointing ozone DIALs in the boundary layer, the natural variability of the ozone concentration in space and time is generally the limiting factor for the assessment of accuracy. This is due to the difficulty in probing the DIAL measurement volume with similar sampling properties in both space and time. In particular, DIAL systems integrate their measurements over an approximately cylindrical sample volume, while *in situ* instruments sample only at one inlet location. In addition, it is difficult to position *in situ* instruments in or near the DIAL measurement volume. Previous intercomparison studies have used free flying and tethered balloons, helicopters, airplanes, and adjacent mountain stations for this purpose. One intercomparison strategy puts special emphasis on the intercomparison of time averages and variances at one or several fixed altitudes (Grabbe et al., 1996). Due to the influence of wind, not only temporal but also spatial averaging is achieved. This strategy is limited to the use of constant altitude platforms for the *in situ* instrument, such as tethered

balloons, helicopters, towers, or airplanes. Restricting intercomparisons to relatively homogeneous atmospheric conditions can result in artificially good results as some systematic errors for both DIAL and *in situ* measurements occur only in the presence of strong atmospheric gradients.

A very simple, but practical piece of advice is to compare ozone concentrations in the dimension of number or mass densities. This corresponds to units of m^{-3} or $\mu\text{g}/\text{m}^3$. For all instruments these are the quantities which are directly measured. At a later point, ozone concentrations may be converted to the more commonly used mixing ratios (i.e., ppb). This conversion involves the additional knowledge of atmospheric density or of temperature and pressure at the measurement location. While trivial, this conversion introduces additional errors from pressure and temperature measurements (or models) which, in practice, can be sizable (e.g., Hilsenrath et al., 1986).

5.5.3 Aloft Performance Audits

Aloft performance audits for aircraft and balloon based instrumentation complement ground based performance audits. They take place in the same setting as the actual measurements and are able to identify some problems which are not noticed in ground based audits, such as problems related to air speed, altitude, and vibrations. For ozone lidar systems, aloft performance audits constitute the only meaningful kind of performance audit, making them a necessity.

The aloft performance audits for SCOS97 are not true performance audits as no primary standard is being used but take the form of intercomparison studies. The ideal lidar location for such a study is adjacent to an air quality monitoring station for ground based intercomparison, close to an ozonesonde launch site, and close to an airport, so that airborne *in situ* ozone measurements can be extended to ground level.

As part of SCOS97, the Desert Research Institute (DRI) is organizing an aloft performance audit, prior to the main study. This performance audit will be conducted in the vicinity of El Monte Airport (EMA) with the airport serving as base. Aloft intercomparisons between the NOAA ozone lidar (located at EMA), CE-CERT ozonesondes and several instrumented aircraft (UCD, STI, Gibbs Cessna, and NAVY EOPACE) will be included in this audit. In addition, the availability of upper air meteorological data is important to improve the comparison between different sample volumes. Data from the RWP/RASS system located at EMA will be utilized for this purpose.

Three flight patterns for the participating aircraft will be utilized for this performance audit:

- Spiral flight patterns (Figure 5-1) will be used for the intercomparison between aircraft themselves, and between aircraft, ozone lidar, and ozonesondes. This is the most generally useful flight pattern for intercomparison.
- Spiral flight patterns interspersed with orbits (Figure 5-2) will be used for the intercomparison between a single aircraft and the ozone lidar. The additional orbits

make it possible to distinguish between horizontal and vertical gradients encountered by an aircraft flying a spiral pattern.

- Traverses will be used for additional intercomparison between the different instrumented aircraft.

The aloft performance audit will take place prior to the main study during the week of June 9, 1997. Conducting the audit before the main study will make it possible to identify, address, and possibly correct potential performance problems prior to commencement of the main study period.

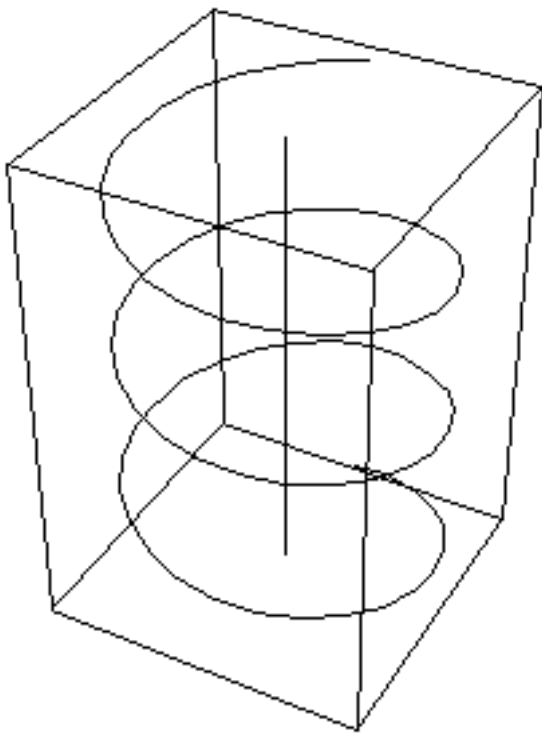


Figure 5-1: Spiral flight pattern, centered on laser beam

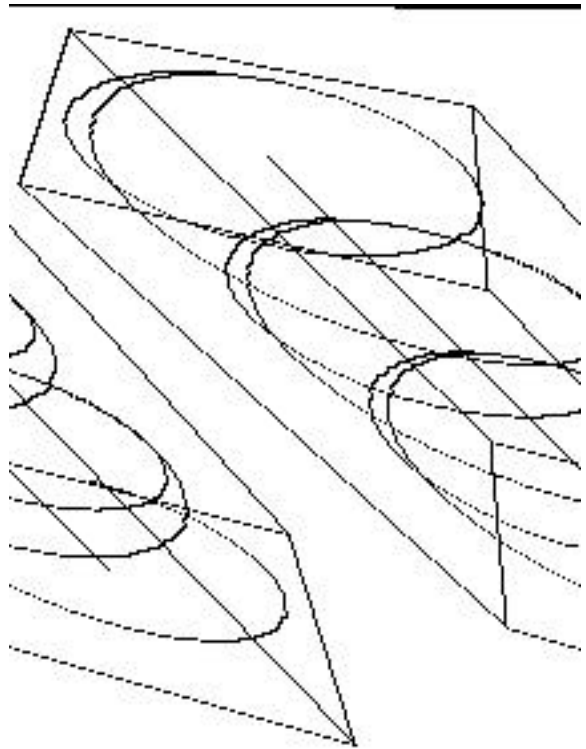


Figure 5-2: Spiral flight pattern interspersed with constant altitude orbits

The NOAA lidar is scheduled to be on-line by June 9, 1997 and it is planned to have all participating aircraft stationed at EMA during this week. The actual intercomparison day will be selected according to recommendations from the forecast team, which will be asked to begin forecasts at least a week before commencement of the main study period. If possible, a high pollution day will be chosen for the intercomparisons. Atmospheric conditions on high pollution days are more likely to resemble those during intensive study periods, making the intercomparison

more relevant to the measurements during the main study. This is especially significant for ozone lidar and ozonesondes, which can suffer from aerosol and oxidant interferences, respectively.

Spatial and Temporal Resolutions

The aircraft used for upper-air air quality measurements travel with a horizontal speed of about 50 m/s and make ascents or descents with a vertical speed of about 150 m/min. Gas analyzers used aboard of these aircraft have a time resolution of about 15 s. This corresponds to a horizontal resolution of about 750 m and a vertical resolution of about 40 m. Spirals and orbits will be near circular projected on a horizontal plane and have a diameter of about 2 km. This corresponds to a circumference of about 6 km, which takes about 2 min per revolution.

The NOAA ozone lidar operates with a range resolution of about 50 m. This corresponds to a vertical resolution of about $50 \text{ m} \times \cos \theta$, where θ is the angle between the vertical and the pointing direction of the lidar system. Therefore the vertical resolution for zenith looking operation is about 50 m.

The ozone analyzer aboard the CE-CERT ozonesondes has a time resolution of about 1 min. Combined with a typical ascent rate of 180 m/min this results in a vertical resolution of about 180 m, less than either lidar or aircraft profiles. The ozonesonde ascent rate is nearly identical to aircraft ascent rates.

Spiral Flight Patterns for Intercomparison between Aircraft, Ozone Lidar, and Ozonesondes

Spiral flight patterns will be used for the intercomparison between aircraft themselves, and between aircraft, ozone lidar, and ozonesondes. This is the most generally useful flight pattern for intercomparison. An idealized example is shown in Fig. 5-1. Here the airplane spirals around the zenith pointing laser beam of the ground based ozone lidar system. Airplane flight patterns are designed taking the temporal resolution of the *in situ* instruments as well as the temporal and spatial resolution of the DIAL system into account.

Specifically, circular spirals with 2 km diameter, centered on the ozone lidar location will be flown. Most spirals will extend from ground level (takeoff or landing) to about 3000 m AGL. At an ascent/descent rate of 150 m/min flying one spiral will take about 20 min. Individual aircraft will be spaced 2 min in time, corresponding to 300 m in altitude. This spacing takes the need for both flight safety and near simultaneous measurements into account.

Spiral flight patterns will be flown with the ozone lidar zenith pointing and with the ozone lidar scanning in a one-dimensional plane. The scanning data will verify lidar performance in this mode of operation and yield data about horizontal atmospheric gradients.

Two ozonesonde releases will be conducted during the spiral intercomparison with the ozone lidar in zenith pointing mode for one release and in scanning mode for the other. Ideally, the ozone lidar would be scanning in a plane parallel to the wind direction. This plane would include the ascent path of the ozonesonde for comparison with the ozonesonde data. In practice, the lidar scanning plane cannot be change readily and such an agreement would be coincidental. However, the high temporal resolution of the lidar in connection with wind profiler data could possibly be used to estimate lidar measured ozone concentrations in the ascent path of the ozonesonde.

To transform the *in situ* airplane data into a vertical profile, one assumes horizontal homogeneity over the spiral area. This assumption is frequently not justified, for example inhomogeneous conditions were observed for some spirals during the COAST study (Moosmüller, 1994). An example of the difficulties in comparing *in situ* spiral data with DIAL data has been discussed for the Davis, CA intercomparison experiment in 1993 (Zhao et al., 1994). To evaluate and eliminate these potential problems spiral flight patterns interspersed with orbits have been added to the performance audit and are discussed in the following section.

Spiral Flight Patterns Interspersed with Orbits for Intercomparison between Aircraft and Ozone Lidar

A modified spiral pattern is shown in Fig. 5-2. Here the airplane flies a spiral around the laser beam, interspersed with orbits at multiple altitudes. These orbits give a check on the assumption of horizontal homogeneity over the spiral area. Each orbit will be flown over a duration longer than the time resolution of the ozone DIAL system. In this fashion horizontal inhomogeneities can be averaged out. Circles flown over substantial longer times allow not only comparisons of time averaged data, but also comparison of time evolution and variances. This type of flight pattern allows not only for better quality assurance of the *in situ* vertical profiles but also for extended comparison at several altitudes. Details of the actual flight take into account DIAL and *in situ* spatial and temporal resolutions, airplane capabilities, and of course FAA regulation.

Specifically, the following orbits will be integrated into a spiral: three orbits at 300 m AGL, three orbits at 600 m AGL, three orbits at 1200 m AGL, and three orbits at 2400 m AGL. Each of these spiral-orbit ascents or descents will take about 45 min; 20 min for ascend or descend over 3000 m and 24 min for a total of twelve orbits at 2 min each. The maximum height AGL agrees with the approximate maximum range of the ozone lidar.

Some spiral-orbit flight patterns will be flown with the ozone lidar zenith pointing and some with the ozone lidar scanning in a one-dimensional plane. The scanning data will verify lidar performance in this mode of operation and yield additional data about horizontal atmospheric gradients.

Traverse Flight Patterns for Intercomparison between Aircraft

Traverses will provide additional intercomparison between the different instrumented aircraft. Traverses will include constant altitude sections, ascents, and descents. Traverses will be flown in the lidar scanning plane with the individual aircraft flying side-by-side at safe distances from each other.

Strawman Measurement Program for Aloft Intercomparison

This measurement schedule consists of one flight for aloft intercomparison between all four aircraft, ozonesondes (two releases) and the NOAA ozone lidar in both zenith pointing and scanning operation. This flight will take place in the morning hours when it is likely that stronger gradients in pollutant concentration and other atmospheric parameters exist and the wind speed is expected to be lower. Strong atmospheric gradients yield a more meaningful intercomparison incorporating a variety of conditions. Low wind speeds result in a more vertical ascent path for the ozonesondes, resulting in better spatial overlap with lidar and aircraft measurements. The

flight plan consists of two spirals (one up and one down, between ground level and 3000 m AGL), one ascending traverse (from 500 m AGL to 3000 m AGL), one descending traverse (from 3000 m AGL to 500 m AGL) and two level traverses (at 500 m AGL and at 3000 m AGL). Ozonesondes will be released during both the ascending and the descending spiral. The ozone lidar will be operated in zenith pointing mode during the ascending spiral and in scanning mode thereafter. A sketch of the flight plan is shown in Figure 5-3 and an idealized schedule is given in the following. All altitudes refer to AGL at El Monte Airport.

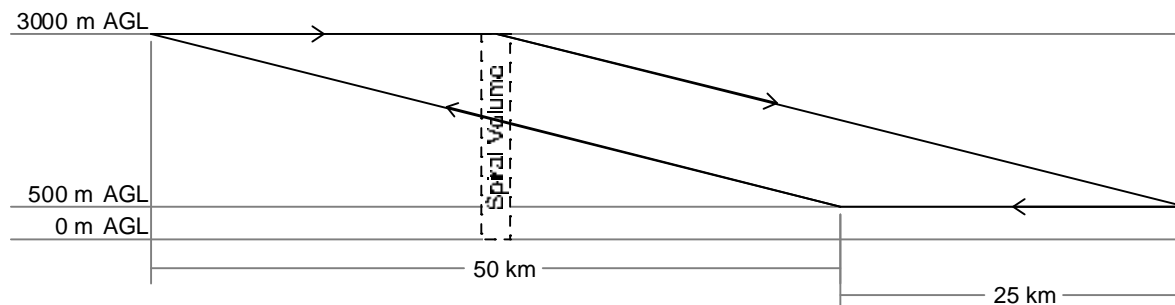


Figure 5-3. Flight plan for airplane intercomparison.

Intercomparison schedule for four aircraft, two ozonesondes, and the NOAA ozone lidar

06:30 PDT	Ozone lidar starts operating in zenith pointing mode
07:00 PDT	First airplane takes off and starts spiral
07:02 PDT	Second airplane takes off and starts spiral
07:04 PDT	Third airplane takes off and starts spiral
07:04 PDT	Ozonesonde release at El Monte
07:06 PDT	Fourth airplane takes off and starts spiral
07:20 PDT	First airplane arrives at 3000 m AGL at top of spiral
07:22 PDT	Second airplane arrives at 3000 m AGL at top of spiral
07:24 PDT	Third airplane arrives at 3000 m AGL at top of spiral
07:26 PDT	Fourth airplane arrives at 3000 m AGL at top of spiral
07:27 PDT	All airplanes start descending traverse to 500 m AGL
07:44 PDT	At 500 m AGL all airplanes start level traverse
07:45 PDT	Ozone lidar switches to scanning mode
07:52 PDT	All airplanes start ascending traverse from 500 m AGL to 3000 m AGL
08:09 PDT	At 3000 m AGL above El Monte, first airplane starts descending spiral
08:11 PDT	At 3000 m AGL above El Monte, second airplane starts descending spiral

08:13 PDT	At 3000 m AGL above El Monte, third airplane starts descending spiral
08:15 PDT	At 3000 m AGL above El Monte, fourth airplane starts descending spiral
08:23 PDT	Ozonesonde release at El Monte
08:29 PDT	First airplane lands
08:31 PDT	Second airplane lands
08:33 PDT	Third airplane lands
08:35 PDT	Fourth airplane lands
09:05 PDT	Ozone lidar stops operating

The next two flights on the same day will intercompare the measurements from one instrumented aircraft (UCD Cessna 182) with those from the NOAA ozone lidar. Each flight will incorporate two spirals and two spiral-orbits taking a total of 2 hours and 10 minutes. During one flight the lidar will be operated in scanning mode, during the other in zenith pointing mode. Idealized schedules are given in the following.

Intercomparison schedule for UCD aircraft and the NOAA ozone lidar in scanning mode

10:05 PDT	Ozone lidar starts operating in scanning mode
10:35 PDT	UCD airplane takes off and starts spiral
10:55 PDT	UCD airplane arrives at 3000 m AGL at top of spiral
10:55 PDT	UCD airplane starts descending spiral-orbit with three orbits each at 2400 m, 1200 m, 600 m and 300 m
11:40 PDT	UCD airplane arrives at or near ground level
11:40 PDT	UCD airplane starts ascending spiral-orbit with three orbits each at 300 m, 600 m, 1200 m and 2400 m
12:25 PDT	UCD airplane arrives at 3000 m AGL at top of spiral-orbit
12:25 PDT	UCD airplane starts descending spiral
12:45 PDT	UCD airplane lands
13:15 PDT	Ozone lidar stops operating

Intercomparison schedule for UCD aircraft and the NOAA ozone lidar in zenith pointing mode

14:15 PDT	Ozone lidar starts operating in zenith pointing mode
14:45 PDT	UCD airplane takes off and starts spiral
15:05 PDT	UCD airplane arrives at 3000 m AGL at top of spiral

15:05 PDT	UCD airplane starts descending spiral-orbit with three orbits each at 2400 m, 1200 m, 600 m and 300 m
15:50 PDT	UCD airplane arrives at or near ground level
15:50 PDT	UCD airplane starts ascending spiral-orbit with three orbits each at 300 m, 600 m, 1200 m and 2400 m
16:35 PDT	UCD airplane arrives at 3000 m AGL at top of spiral-orbit
16:35 PDT	UCD airplane starts descending spiral
16:55 PDT	UCD airplane lands
17:25 PDT	Ozone lidar stops operating